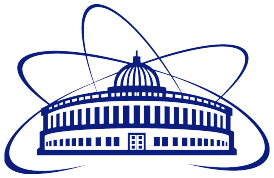

JOINT INSTITUTE FOR NUCLEAR RESEARCH

Veksler and Baldin Laboratory of High Energy Physics

FINAL REPORT ON THE START PROGRAMME

Particle Production in UrQMD Model in Au+Au Collisions at $\sqrt{s_{NN}} = 3$ GeV

Student:
Abdulrahman Tarek, Egypt
The American University in Cairo

Supervisor:
Vinh Luong

Participation period:
July 06 – August 30, 2025
Summer Session 2025

Dubna
2025

Abstract

Understanding strangeness production in heavy-ion collisions is essential for exploring the properties of strongly interacting matter in the baryon-rich regime, where hadronic interactions dominate and QCD matter exhibits unique features. In this work, we analyze Λ^0 hyperon transverse-momentum and rapidity distributions in Au+Au collisions at $\sqrt{s_{NN}} = 3$ GeV using the UrQMD transport model, covering multiple collision centralities. The comparison with STAR experimental data shows that UrQMD successfully reproduces key patterns of strange baryon production, validating its applicability at low energies. These findings provide insight into the dynamics of dense nuclear matter, highlighting the role of microscopic transport approaches in studying strangeness as a probe of hadronic matter properties.

Contents

1 Introduction

1.1 The QCD Phase Diagram and the Quark-Gluon Plasma

The Quantum Chromodynamics (QCD) phase diagram (Fig. 1), typically represented in terms of temperature (T) versus baryonic chemical potential (μ_B), encodes the various states of strongly interacting matter [1]. At sufficiently high temperatures and energy densities, hadronic matter undergoes a transition to a deconfined state of quarks and gluons, known as the Quark-Gluon Plasma (QGP) [2]. This state is believed to have existed microseconds after the Big Bang and can be recreated in relativistic heavy-ion collisions at RHIC and LHC [3]. Understanding the QGP provides insight into the equation of state of nuclear matter and the dynamics of confinement-deconfinement transitions.

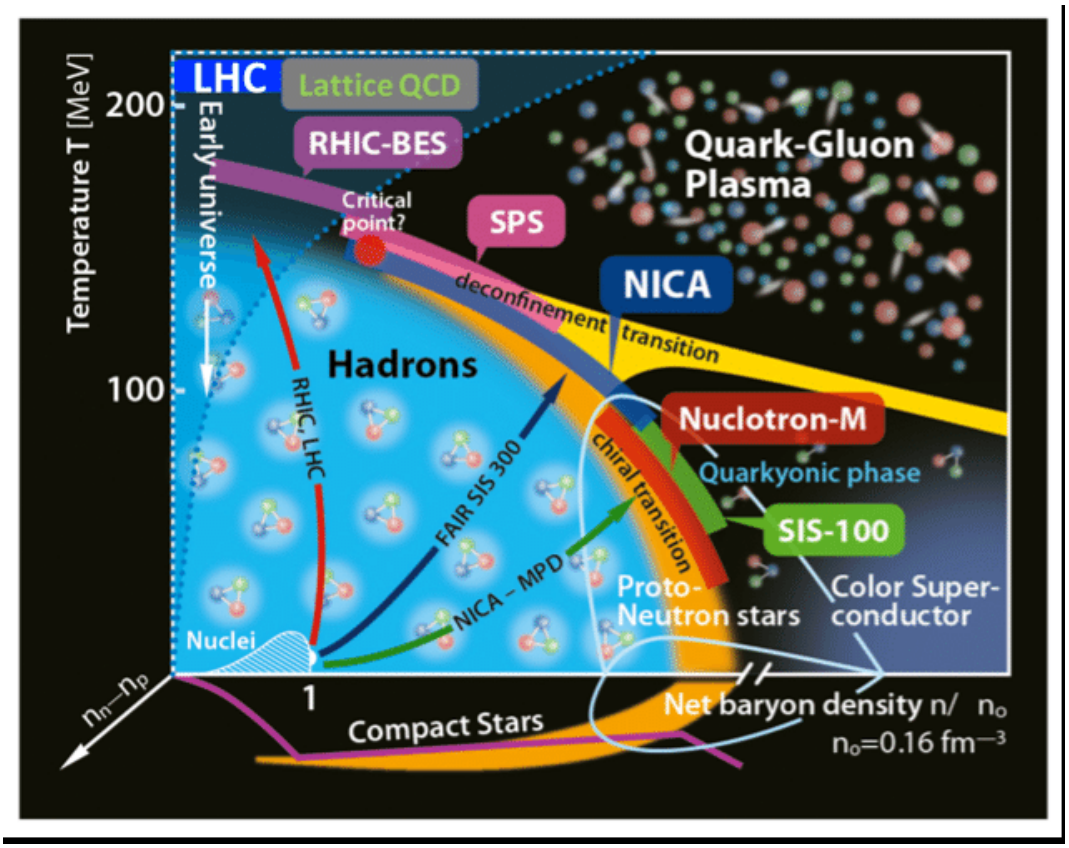

Figure 1: Schematic representation of the QCD phase diagram illustrating hadronic matter and the Quark-Gluon Plasma.

1.2 Scope of the Work

This work focuses on the production of Λ^0 hyperons in Au+Au collisions at $\sqrt{s_{NN}} = 3$ GeV. Using UrQMD simulations, we analyze transverse momentum and rapidity spectra for several centrality classes and compare the results with STAR experimental data. The goal is to assess the performance of UrQMD in describing strange baryon production at low energies and to provide insights into the dynamics of baryon-rich matter.

1.3 Λ^0 Hyperon

The Λ^0 hyperon, consisting of up, down, and strange quarks (uds), is the lightest neutral strange baryon. Its relatively long lifetime and characteristic weak decay modes, such as

$$\Lambda^0 \rightarrow p + \pi^- \tag{1}$$

make it experimentally accessible. Studying Λ^0 production provides information on strangeness equilibration, particle production mechanisms, and the behavior of baryon-rich matter in low-energy heavy-ion collisions.

2 STAR Experiment Setup

In this study, Au+Au collision data at $\sqrt{s_{NN}} = 3$ GeV were collected using STAR's fixed-target mode during the 2018 RHIC run [10], Fig. 2 shows the layout of the STAR experiment setup. A single gold beam of energy 3.85 GeV/nucleon collided with a stationary gold target placed 2 cm below the beam axis inside the vacuum pipe. The target thickness corresponded to approximately 1% interaction probability. The setup enabled access to the high-baryon-density regime ($\mu_B \approx 500$ MeV), exploring regions of the QCD phase diagram relevant to dense nuclear matter. Strange hadrons such as K^0_S and Λ^0 were measured by STAR [10] via their weak decay channels, and the data were analyzed across multiple centrality and rapidity bins.

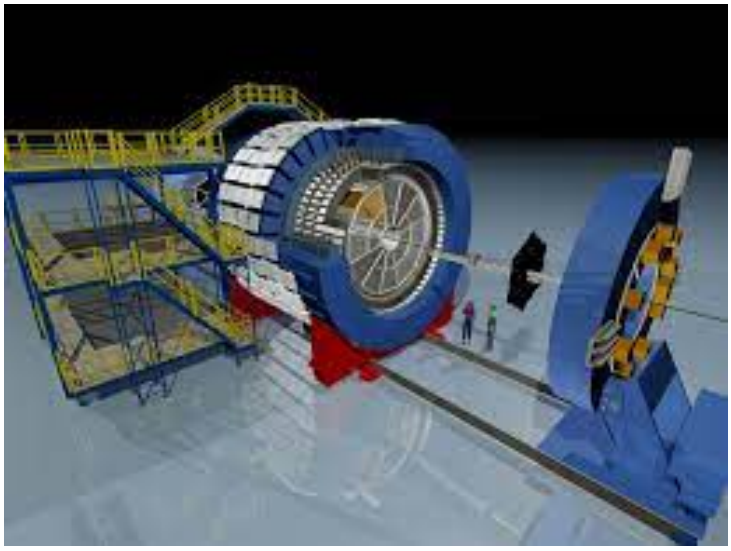

Figure 2: The layout of the STAR experiment setup.

3 UrQMD Model

The Ultra-relativistic Quantum Molecular Dynamics (UrQMD) model [4, 5] is a microscopic transport approach widely used to simulate heavy-ion collisions across a broad range of energies. UrQMD propagates hadrons classically while modeling stochastic interactions such as elastic and inelastic scattering, resonance formation and decay, and string excitation at higher energies. By tracking the full phase-space evolution of hadrons during the collision, UrQMD enables detailed studies of particle production, collective flow, and strangeness dynamics.

The initialization of nuclei and the incorporation of fermionic effects rely on concepts from Fermionic Molecular Dynamics [6] and Pauli-principle-based many-body models [7], with stochastic sampling methods such as the Metropolis algorithm [8] used for phase-space configurations. Resonance properties and particle data are taken from experimental compilations [9] to ensure realistic reproduction of hadron yields and spectra.

4 Results

In this section, we compare the production of Λ^0 hyperons in Au+Au collisions at $\sqrt{s_{NN}} = 3.0$ GeV between experimental measurements from the STAR experiment and simulations performed with the UrQMD model. The comparison is presented in terms of transverse momentum (p_T) spectra and rapidity (y) distributions across six centrality classes: [0–10%], [10–20%], [20–30%], [30–40%], [40–60%], and [60–80%]. The experimental data points are taken from [10].

For a consistent comparison, the UrQMD simulations are analyzed using the same kinematic cuts and binning as the experimental measurements. This ensures that the model predictions can be directly contrasted with the STAR results, providing insight into the ability of UrQMD to describe strange baryon production at low beam energies.

4.1 Transverse momentum distributions

The transverse momentum (p_T) spectra of Λ^0 hyperons for the six centrality intervals, shown in Figures 3–8, display the expected exponential trend characteristic of particle production in low-energy heavy-ion collisions. The UrQMD calculations reproduce the overall shape and magnitude of the experimental distributions across all centralities, exhibiting good agreement with STAR measurements within statistical uncertainties.

In the most central collisions [0–10%], the model captures both the low- and intermediate-p_T behavior, reflecting a realistic description of baryon transport and collective effects. For mid-central events ([10–20%], [20–30%]), the simulation continues to describe the spectral slopes accurately, although slight deviations appear at very low p_T, consistent with the finite resolution of the model in reproducing soft particle production. In peripheral collisions ([30–40%], [40–60%], [60–80%]), the agreement remains robust across the full p_T range, confirming that UrQMD effectively reproduces the overall centrality dependence of Λ^0 production.

These observations suggest that the transport approach implemented in UrQMD reliably accounts for the essential features of strangeness production and the underlying dynamics governing the transverse momentum distributions at $\sqrt{s_{NN}} = 3$ GeV.

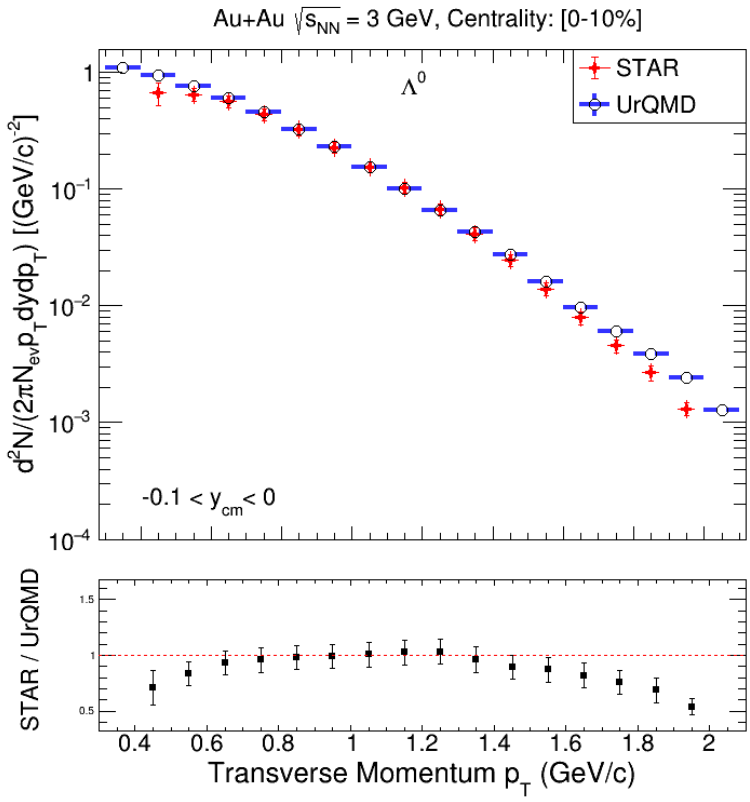

Figure 3: Transverse-momentum spectra of Λ^0 for centrality [0–10%] comparing STAR data and UrQMD simulation; lower panel shows the ratio.

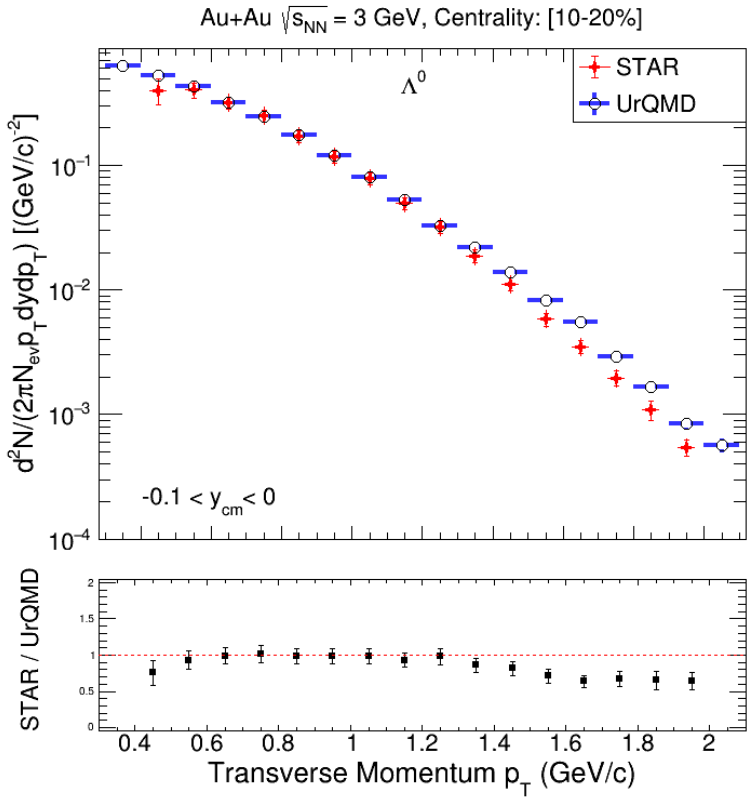

Figure 4: Transverse-momentum spectra of Λ^0 for centrality [10–20%] comparing STAR data and UrQMD simulation; lower panel shows the ratio.

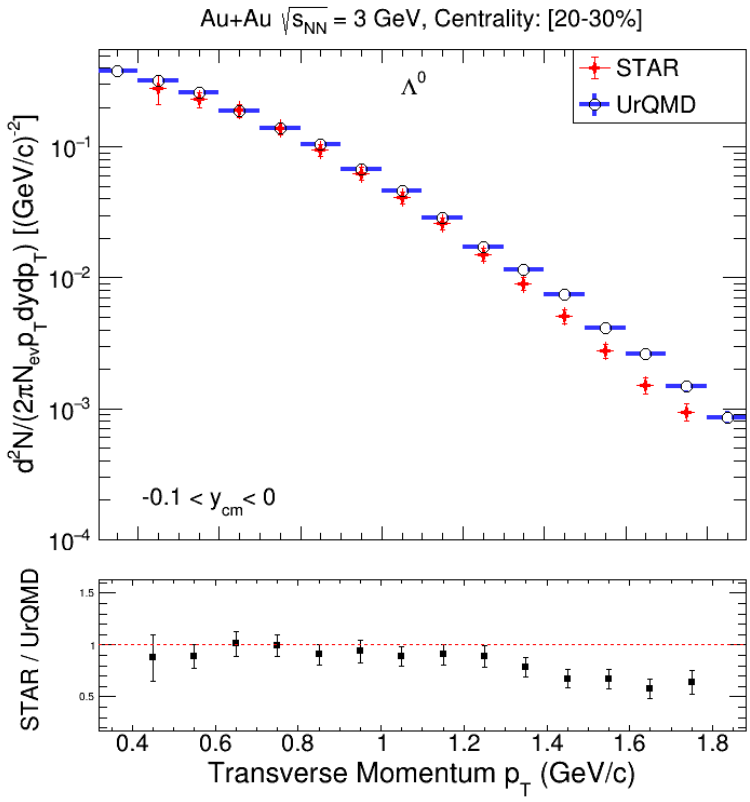

Figure 5: Transverse-momentum spectra of Λ^0 for centrality [20–30%] comparing STAR data and UrQMD simulation; lower panel shows the ratio.

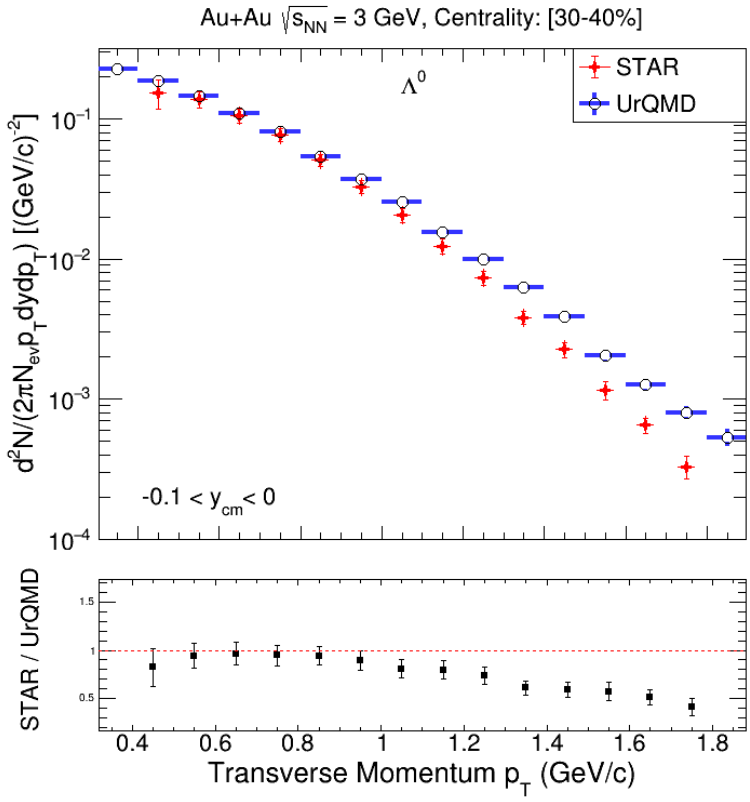

Figure 6: Transverse-momentum spectra of Λ^0 for centrality [30–40%] comparing STAR data and UrQMD simulation; lower panel shows the ratio.

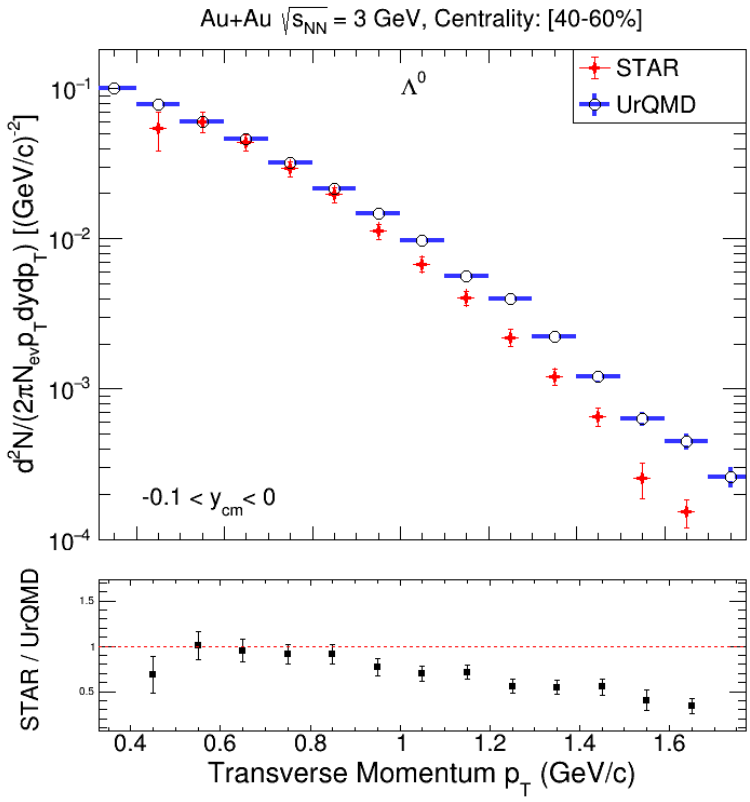

Figure 7: Transverse-momentum spectra of Λ^0 for centrality [40–60%] comparing STAR data and UrQMD simulation; lower panel shows the ratio.

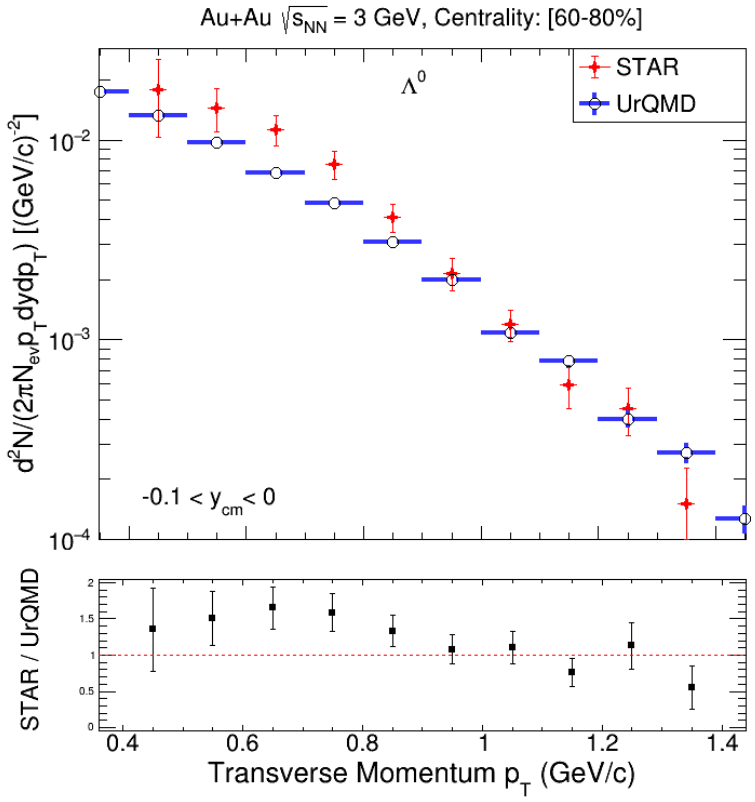

Figure 8: Transverse-momentum spectra of Λ^0 for centrality [60–80%] comparing STAR data and UrQMD simulation; lower panel shows the ratio.

4.2 Transverse Momentum Spectra for Multiple Species and Centralities

To complement the comparison of UrQMD calculations with STAR measurements, we performed an extended analysis of the model output. In particular:

- The transverse momentum (p_T) spectra of Λ^0 baryons were plotted for all six centrality classes ([0–10%], [10–20%], [20–30%], [30–40%], [40–60%], [60–80%]) on a single figure as shown in Figure 9 to provide a clear overview of centrality dependence in UrQMD simulations.

  The trend that central collisions ([0–10%]) produce particles with higher average transverse momentum (p_T) than mid-central ([10–30%]) and peripheral collisions ([30–80%]) can be explained by the geometry and energy density of the interaction zone [11]. In central collisions, the nuclei overlap almost completely due to the small impact parameter (b), creating a dense system with many participating nucleons (N_{part}) and strong collective effects, which push particles to higher p_T. Peripheral collisions, on the other hand, involve only a small overlap and fewer participants, leading to lower energy density and softer p_T spectra. This centrality dependence of p_T is consistent with the well-established picture in heavy-ion physics [11].

- We analyzed the transverse momentum (p_T) spectra of five identified particle species produced in Au+Au collisions at $\sqrt{s_{NN}} = 3.0$ GeV using the UrQMD model: protons (p), charged pions ($\pi^{\pm}$), and charged kaons ($K^{\pm}$), as shown in Figure 10.

  The yield of K^+ is higher than that of K^- at these energies due to *associated production* processes [12, 13], for example,

  $$N + N \to \Lambda^0 + K^+ + N,$$

  where a K^+ is produced together with a Λ^0 hyperon. The high baryon density in central collisions favors K^+ production, while K^- is suppressed due to the absence of similar production channels [12].

  For pions, the neutron excess in gold nuclei ($N > Z$) naturally leads to more π^- than π^+, reflecting the isospin asymmetry of the system [14].

- These plots provide additional insight into the relative production of strange and non-strange hadrons and allow for a qualitative assessment of model performance across particle species.

The inclusion of these additional spectra helps to validate UrQMD's overall description of particle production and provides a more comprehensive baseline for future comparison with experimental data.

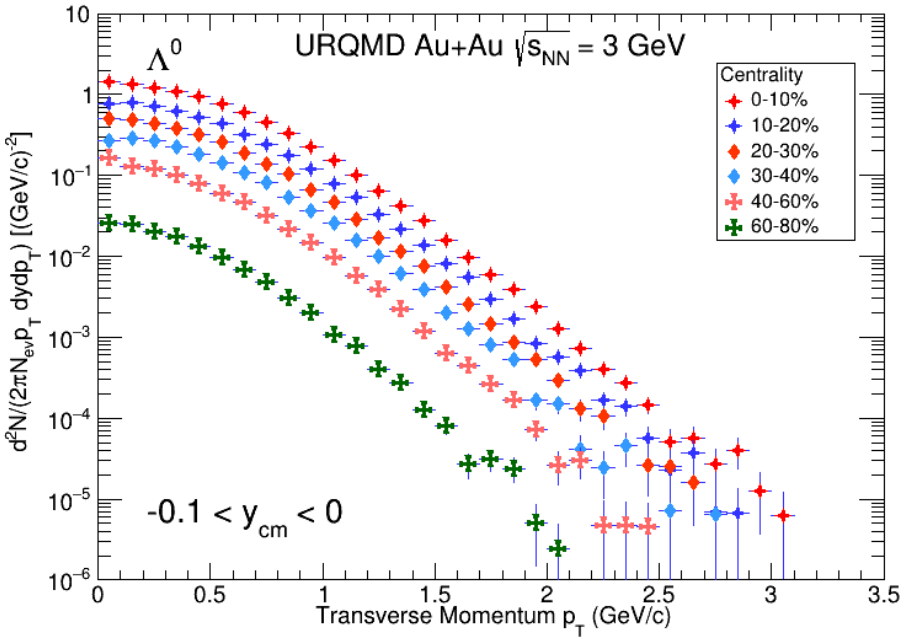

Figure 9: Transverse momentum (p_T) spectra of Λ^0 baryons from UrQMD simulations of Au+Au collisions at $\sqrt{s_{NN}} = 3.0$ GeV for six centrality classes ([0–10%], [10–20%], [20–30%], [30–40%], [40–60%], [60–80%]). Statistical uncertainties are shown as vertical bars.

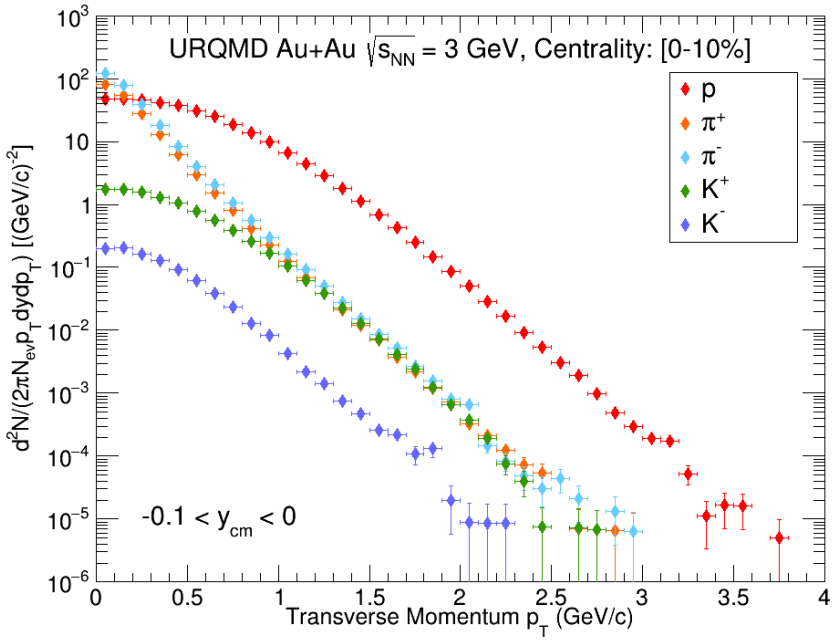

Figure 10: Transverse momentum (p_T) spectra of identified hadrons from UrQMD simulations of Au+Au collisions at $\sqrt{s_{NN}} = 3.0$ GeV: protons (p), positively and negatively charged pions (π^+, π^-), and positively and negatively charged kaons (K^+, K^-). Spectra are shown for minimum-bias events. Statistical uncertainties are shown as vertical bars.

4.3 Rapidity distributions

Figures 11–16 present the rapidity (dN/dy) distributions of Λ^0 baryons for the same centrality intervals. The distributions are approximately Gaussian, peaking at mid-rapidity ($y = 0$), with the overall normalization decreasing from central to peripheral collisions, consistent with the collision geometry.

UrQMD reproduces the general Gaussian shape of the dN/dy distributions. However, similar to the p_T spectra, the model tends to underestimate the Λ^0 yield at mid-rapidity in central collisions, while achieving closer agreement in peripheral bins. The width of the rapidity distributions predicted by UrQMD is comparable to the STAR data, indicating that the model captures the longitudinal dynamics of the system reasonably well at this beam energy.

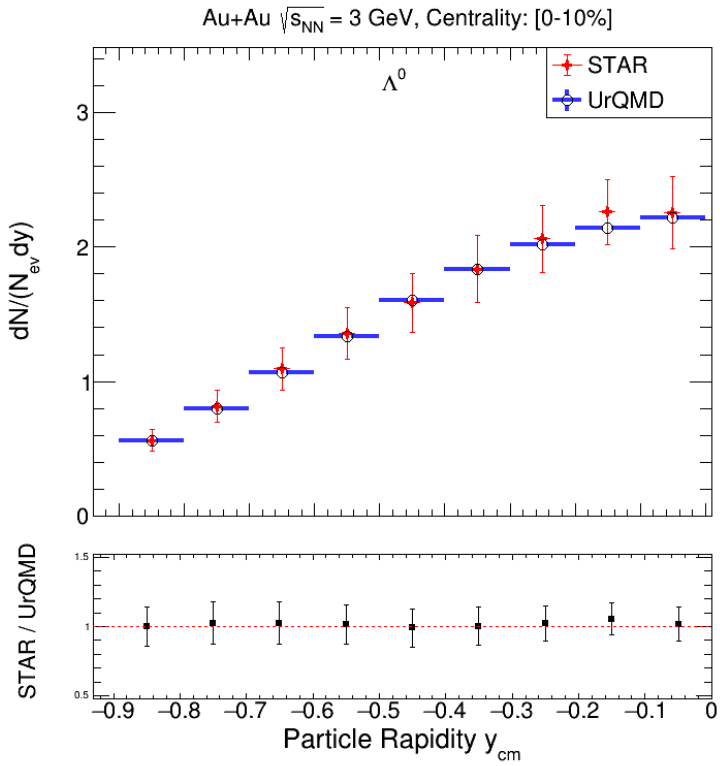

Figure 11: Rapidity distributions of Λ^0 for centrality [0–10%] comparing STAR data and UrQMD simulation; lower panel shows the ratio.

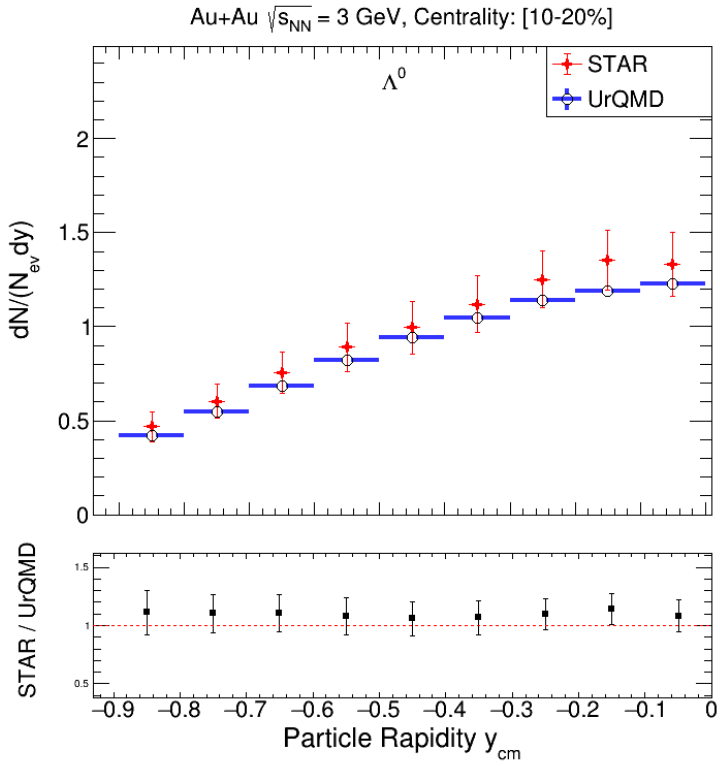

Figure 12: Rapidity distributions of Λ^0 for centrality [10–20%] comparing STAR data and UrQMD simulation; lower panel shows the ratio.

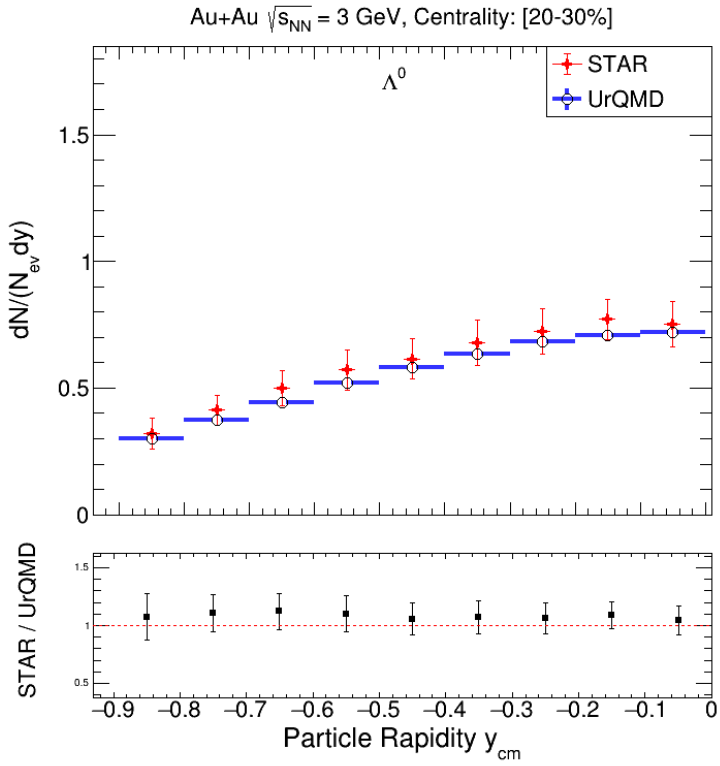

Figure 13: Rapidity distributions of Λ^0 for centrality [20–30%] comparing STAR data and UrQMD simulation; lower panel shows the ratio.

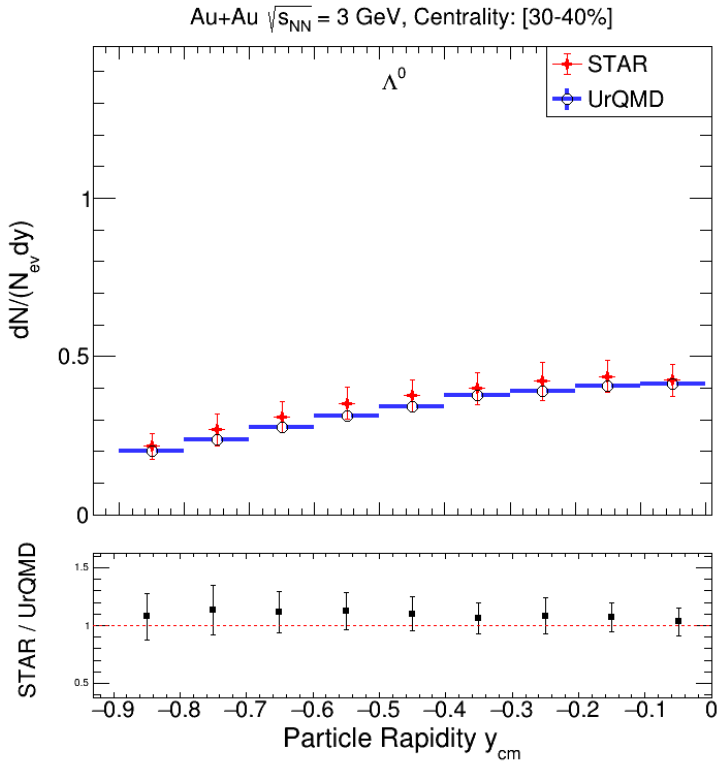

Figure 14: Rapidity distributions of Λ^0 for centrality [30–40%] comparing STAR data and UrQMD simulation; lower panel shows the ratio.

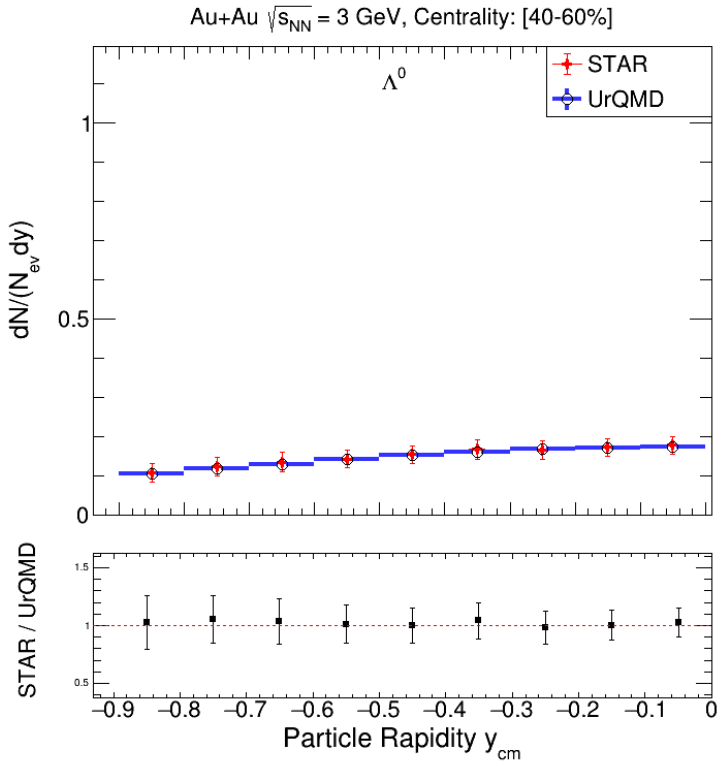

Figure 15: Rapidity distributions of Λ^0 for centrality [40–60%] comparing STAR data and UrQMD simulation; lower panel shows the ratio.

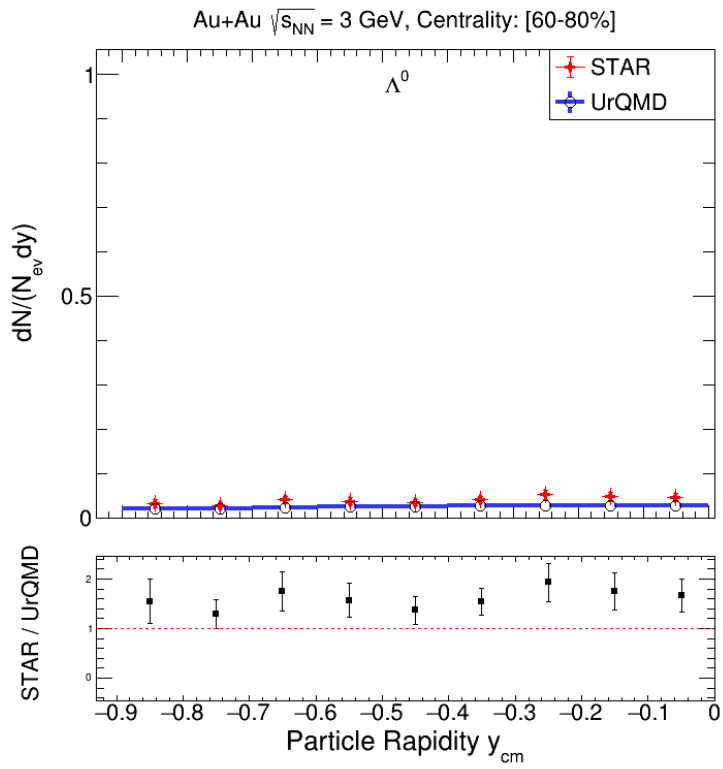

Figure 16: Rapidity distributions of Λ^0 for centrality [60–80%] comparing STAR data and UrQMD simulation; lower panel shows the ratio.

5 Conclusion

In summary, we presented a comparative study of Λ^0 production in Au+Au collisions at $\sqrt{s_{NN}} = 3.0$ GeV, analyzing UrQMD transport model simulations against STAR experimental data across six centrality classes. The transverse momentum (p_T) spectra and rapidity (dN/dy) distributions show a clear centrality dependence, with yields decreasing systematically from central to peripheral collisions.

The UrQMD model qualitatively reproduces the shapes of both p_T spectra and rapidity distributions, reflecting the hadronic dynamics expected in the baryon-rich regime. However, discrepancies remain—most prominently, the underestimation of Λ^0 yields at low p_T in central collisions—indicating that additional mechanisms may be required in the model description.

We also presented extended results from UrQMD, including (i) a combined comparison of Λ^0 spectra across all six centrality classes, and (ii) transverse momentum spectra of other hadron species (p, π^+, π^-, K^+, K^-) at [0–10%] centrality. These provide further benchmarks for testing the performance of hadronic transport models at low collision energies.

Overall, the comparison demonstrates that UrQMD captures several qualitative features of Λ^0 production, but systematic differences with STAR data highlight the need for further model refinement.

Acknowledgments

I sincerely thank my supervisor, Vinh Luong, for his invaluable guidance, support, and constructive feedback throughout this project. I am also grateful to the staff at JINR's Veksler and Baldin Laboratory of High Energy Physics (VBLHEP) for their assistance and encouragement. This work was made possible through the JINR Summer Student Programme, which provided an excellent research environment as well as financial support, including travel reimbursement, accommodation, and daily allowances.

References

[1] B. Müller, *The Physics of the Quark-Gluon Plasma*, Cambridge University Press, 2025, Cambridge University Press link.

[2] E. Itou, *Recent Progress in Lattice QCD Studies of the Quark-Gluon Plasma*, Prog. Part. Nucl. Phys. **120** (2025) 103900, DOI:10.1016/j.ppnp.2021.103900.

[3] STAR Collaboration, Hui Wang (for the collaboration), *STAR Results from the RHIC Beam Energy Scan*, J. Phys. Conf. Ser. **458** (2013) 012001, DOI:10.1088/1742-6596/458/1/012001.

[4] M. Bleicher *et al.*, *Relativistic hadron-hadron collisions in the ultrarelativistic quantum molecular dynamics model*, J. Phys. G **25** (1999) 1859, DOI:10.1088/0954-3899/25/9/307.

[5] S. A. Bass *et al.*, *Microscopic models for ultrarelativistic heavy-ion collisions*, Prog. Part. Nucl. Phys. **41** (1998) 225, DOI:10.1016/S0146-6410(98)00058-1.

[6] H. Feldmeier, *Fermionic Molecular Dynamics*, Nucl. Phys. A **515** (1990) 147, DOI:10.1016/0375-9474(90)90328-J.

[7] L. Wilets, E. M. Henley, M. Kraft, and A. D. McKellar, *Classical many-body model for heavy-ion collisions incorporating the Pauli principle*, Nucl. Phys. A **282** (1977) 341, DOI:10.1016/0375-9474(77)90220-2.

[8] N. Metropolis, A. W. Rosenbluth, M. N. Rosenbluth, A. H. Teller, and E. Teller, *Equation of State Calculations by Fast Computing Machines*, J. Chem. Phys. **21** (1953) 1087, DOI:10.1063/1.1699114.

[9] Particle Data Group, *Review of Particle Properties*, Phys. Rev. D **54** (1996), DOI:10.1103/PhysRevD.54.1.

[10] STAR Collaboration, *Strangeness Production in* $\sqrt{s_{NN}} = 3$ *GeV Au+Au Collisions at RHIC*, arXiv:2407.10110 (2024), arXiv:2407.10110.

[11] ALICE Collaboration, B. Abelev *et al.*, *Centrality dependence of* π*, K, p production in Pb–Pb collisions at* $\sqrt{s_{\rm NN}} = 2.76$ *TeV*, Phys. Rev. C **88** (2013) 044910, arXiv:1303.0737 [nucl-ex].

[12] C. Fuchs, *Kaon production in heavy ion reactions at intermediate energies*, Prog. Part. Nucl. Phys. **56** (2006) 1–103, arXiv:nucl-th/0507017.

[13] P. Braun-Munzinger, K. Redlich, and J. Stachel, *Particle production in heavy ion collisions*, in R. C. Hwa and X.-N. Wang (eds.), Quark–Gluon Plasma 3, World Scientific (2004) 491–599, arXiv:nucl-th/0304013.

[14] A. Andronic, P. Braun-Munzinger, and J. Stachel, *Hadron production in central nucleus–nucleus collisions at chemical freeze-out*, Nucl. Phys. A **772** (2006) 167–199, arXiv:nucl-th/0511071.